საქართველოს მეცნიერებათა ეროვნული აკადემიის მოამბე, ტ. 17, №1, 2023
BULLETIN OF THE GEORGIAN NATIONAL ACADEMY OF SCIENCES, vol. 17, no. 1, 2023

Physical Chemistry

On High-Temperature Oxidation Kinetics of Alloy FeCr(La): Reduction of the Effective Diffusion Area

Irakli Nakhutsrishvili[*] and Giorgi Mikadze[**]

[*]*Institute of Cybernetics, Georgian Technical University, Tbilisi*
[**]*Georgian Technical University, Tbilisi*

(Presented by Academy Member Vladimer Tsitsishvili)

High-temperature (1300-1400°C) oxidation of FeCr(La) alloy was studied by thermogravimetry. The kinetic dependence of the FeCr(La) mass change has a specific form due to the occurrence of reduction of the reaction surface. This is due to the formation of diffusion barriers from lanthanum chromite $LaCrO_3$. New kinetic dependence of the alloy mass change was tested, which differs from the classical Evans equation. This new equation correctly describes the kinetics of the process. © *2023 Bull. Georg. Natl. Acad. Sci.*

high-temperature oxidation, alloy FeCr(La), decrease of reaction surface

Alloys on an iron-chromium equiatomic basis (chromia-forming alloys) are materials for coating hot components of gas turbine engines. In particular, lanthanum-doped FeCr alloys have high heat resistance up 1300°C to 1400°C. During the oxidation of these alloys, scale $Cr_2O_3$is formed on their surface. The boundaries of oxide grains (the main arteries of mass transfer) in it are blocked by diffusion barriers from chromite $LaCrO_3$. This is equivalent to a decrease in the effective area of the reaction and leads to a deviation of the oxidation kinetics from parabolic [1, 2]. For the processes with the decreased reaction surface, U.R. Evans deduced the following ratio [3]:

$$\varphi \equiv S / S_0 = e^{-km}, \tag{1}$$

where, S_0 is the initial area of metal or alloy surface, and S is the area free from the diffusion barriers of the surface of the specimen in case of mass gain m (mass increase at the expense of the oxygen entered into the reaction), k is the surface reduction coefficient. Based on the parabolic dependence $m^2 = k_p t$ and Eq. (1), the following equation was derived [2, 3]:

$$m = \frac{1}{k}\ln\left(k\sqrt{k_p t} + 1\right), \tag{2}$$

(k_p – parabolic constant, t – time). It was also derived inexplicitly kinetic dependence [4]:

$$t = \frac{2}{k^2 k_p}\left[e^{km}\left(km-1\right)+1\right]+\frac{1}{kk_r}\left(e^{km}-1\right) \tag{3}$$

based on the "complex parabola" $\left(m^2/k_p\right)+\left(m/k_r\right)=t$ or in differential form (taking into account Eq. (1)): $dm/dt = \frac{k_p}{2m+k_p/k_r}e^{-km}$, where $k_r = \frac{dm}{dt}\left|t=0, m=0\right.$ is rectilinear constant. Eq. (3) correctly described the kinetics of air oxidation of Al_2O_3 and Cr_2O_3 – forming alloys doped with lanthanum or yttrium [5, 6]. During the oxidation of Cr_2O_3 -forming alloys, the evaporation of Cr_2O_3 in the form of suboxide CrO_3 also occurs [1]. Therefore, the total mass change is $M=m-v_mt$, where v_m is the rate of evaporation of Cr_2O_3 for the metalic component. $v_m = \frac{q}{q+1}v_p \cong 0.48v_p$ ($q=3M_0/M_{Cr} \cong 0.923$, v_p – evaporation rate of scale). (That's why the plan of evaporation of the basic oxide is: $4Cr+3O_2=2Cr_2O_3$; $2Cr_2O_3+3O_2=4Cr_2O_3$)). The evaporation rate of $LaCrO_3$ are 1–1.5 range lower, which can be ignored.

Results and Discussion

The experiments on air oxidation of an alloy of the Cr-V-Ta-La system were repeated at temperatures of 1300-1400°C. The total content of alloying elements was ~1 wt.%. Chromium was electrolytically refined in hydrogen with nitrogen and carbon contents (~0.006 and 0.008 wt%). (It is known that these elements (N, C, La) noticeably change the parameters of chromium oxidation and affect the conditions for the formation of a protective oxide layer). The ingots were obtained in a water-cooled mold by induction-arc melting in an argon atmosphere and contained ~0.25 wt.% lanthanum. The experiments were carried out on a continuous weighing microbalance mounted in a vacuum setup (sensitivity ~10^{-6}g). The results of weight measurements are presented in Fig. 1. The data obtained are somewhat (but not fundamentally) different from the data of [2]. The values of constants shown in Table 1.

Table 1. The values of constants in Eq. (3)

Temperature, ℃	k, cm^2/mg	k_r, mg/cm^{2}h	k_p, mg^2/cm^{4}h
1300	0.59	2.88	0,95
1350	0.45	7.0	1.95
1400	0.20	$\to\infty$	3.60

Empirical expressions of Eq. (3):

$$t \cong 6.04\left[e^{0.59m}\left(0.59m-1\right)+1\right]+0.59\left(e^{0.59m}-1\right) \qquad (1300^0\text{C})$$

$$t \cong 5.06\left[e^{0.45m}\left(0.45m-1\right)+1\right]+0.32\left(e^{0.45m}-1\right) \qquad (1350^0\text{C})$$

$$t \cong 13.89\left[e^{0.2m}\left(0.2m-1\right)+1\right] \qquad (1400^0\text{C})$$

$$\left[m\right]=mg/cm^2, \left[t\right]=h.$$

Experimental curves in the used scale practically coincides with curves (1)-(3); (a) and (b) are tangents to curves 1' and 2' at the origin of coordinates (the tangent to curve 3 practically coincides with the y-axis): $tg\alpha,\beta=k_r$.

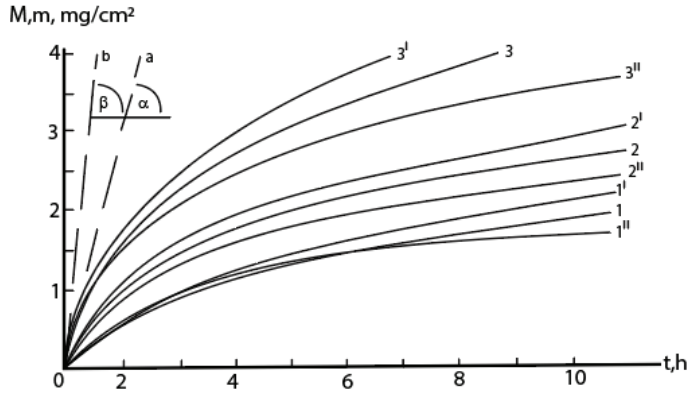

Fig. 1. Curves M=f(t) and m=f(t) at (1, 1') 1300, (2, 2') 1350 and (3, 3') 1400°C. 1'', 2''and 3'' according to Eq. (2).

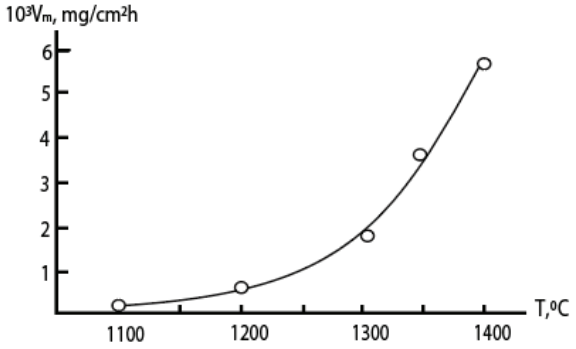

Fig. 2. Evaporation rate of Cr_2O_3 as a function of temperature [1] with the addition of rates at 1350 and 1400°C.

Taking into account expression (1), Eq. (3) can be rewritten as:

$$t = \frac{2}{k^2 k_p}\left[1 - \frac{1}{\varphi}\ln(e\varphi)\right] + \frac{1}{kk_r}\left(\frac{1}{\varphi} - 1\right) \tag{4}$$

and also combining all the above equations, in the first approximation we get that by the moment of practical completion of the formation of diffusion barriers: $\varphi_A \equiv \varphi \left| d\varphi / dt \to 0 \cong e^{(kk_p/2k_r)-1}\right.$. Substituting $\varphi = \varphi_A$ into Eq. (4), we get: $t_A \equiv t_{|\varphi\to\varphi_A} = \frac{2}{k^2 k_p}\left(1 - \frac{kk_p}{2k_r}e^{(1-kk_p/2k_r)}\right) + \frac{1}{kk_r}\left(e^{(1-kk_p/2k_r)} - 1\right)$. The values of φ_A and t_A are given in Table 2.

Table 2. The values of φ_A and t_A

Temperature, ^{0}C	φ_A	t_A, *h*
1300	0.4055≈0.41	5.45
1350	0.392≈0.39	4.75
1400	e^{-1}≅0.368≈0.37	13.90

Fig. 3 shows the kinetic dependences constructed according to Eq. (4). The calculated points φ_A and t_A fit well on the corresponding curves for 1300 and 1350°C. As for 1400°C (at which $k_r \to \infty$), then $\varphi_A \cong e^{-1}$ should be expected at $t_A \cong 2/k^2 k_p \approx 14\ h$.

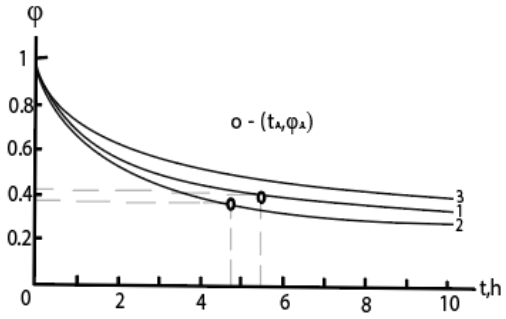

Fig. 3. Kinetic dependences $\varphi - t$ at (1)1300, (2) 1350 and (3) 1400°C.

According to [1, 2], we can conclude that $LaCrO_3$ creates diffusion barriers in the Cr_2O_3 scale. $YCrO_3$ and $CeCrO_3$ have been studied in a number of works ([6-10] and [11-15]). According to [6], $YCrO_3$ also creates diffusion barriers. Thermogravimetric measurements were not carried out in this work. However, a graph based on unpublished data from one of the authors (private notice)can be shown in Fig.4. Section (ac) of curve 1 corresponds to sample heating from room temperature to 1400°C, section (bc) – extrapolation of curve 2. (For construction of calculated curve, product $e^{km_0}(km_0 - 1)$ in Eq. (5) must be given with accuracy 10^{-5}). For the presented curve, instead of Eq.3, should be applied [4]:

$$t = \frac{2}{k^2 k_p}\left[e^{km}\left(km-1\right) - e^{km_0}\left(km_0 - 1\right)\right] + \frac{1}{kk_r}\left(e^{km} - e^{km_0}\right), \tag{5}$$

where $m_0 = m_{|t=0}$. Time shift between Eqs. (3) and (5): $t_0 = \frac{2}{k^2 k_p}\left[e^{km_0}\left(1-km_0\right)-1\right] + \frac{1}{kk_r}\left(1-e^{km_0}\right)$. Empirical expression of Eq. (5): $t \cong 843.313\left[e^{0.022m}\left(0.022m-1\right)-0.999\right] + 14.205\left(e^{0.022m}-1.018\right)$ ($[m]$ = mg/cm^2, $[t]$ = h, $m_0 \cong 0.83$ mg/cm^2 and $t_0 \cong$ -0.43 h).

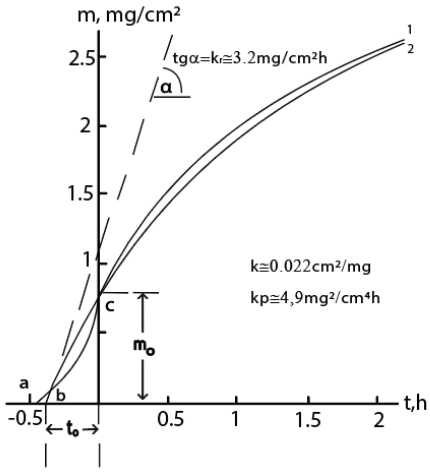

Fig. 4. (1) Experimental kinetic curve of air oxidation of FeCr(Y) at 1400°C; (2) constructed according to Eq. (5) curve.

It can be seen that the curve constructed according to Eq. (5) approaches satisfactorily the experimental one.

For $CeCrO_3$, it can also be assumed that this chromite also creates diffusion barriers. This assumption is supported by the data of the previous work [1]. Undoubtedly, this should be further verified by SEM and TEM methods.

Conclusion

The study of the oxidation process of alloy FeCr(La) in air at 1300-1400°C shows the deviation of the oxidation kinetics from parabolic. This is due to the presence of diffusion barriers from lanthanum chromite $LaCrO_3$ in the scale. The processes of high-temperature oxidation of FeCr(Y) and FeCr(Ce) alloys are also considered. And in these processes, a deviation of the oxidation kinetics from the parabolic one is observed due to the formation of chromites $YCrO_3$ and $CeCrO_3$.

The paper is dedicated to the memory of prof. O.I. Mikadze.

ფიზიკური ქიმია

FeCr(La) შენადნობის მაღალტემპერატურული ოქსიდირების კინეტიკის შესახებ: დიფუზიის ეფექტური ზედაპირის შემცირება

ი. ნახუცრიშვილი* და გ. მიქაძე**

*საქართველოს ტექნიკური უნივერსიტეტი, კიბერნეტიკის ინსტიტუტი, თბილისი
**საქართველოს ტექნიკური უნივერსიტეტი, თბილისი

(წარმოდგენილია აკადემიის წევრის ვ. ციციშვილის მიერ)

თერმოგრავიმეტრიული მეთოდით შესწავლილია ლანთანით ლეგირებული FeCr შენადნობის მაღალტემპერატურული (1300-1400°C) ოქსიდირების კინეტიკა ჰაერზე. ნიმუშთა მასის ცვლილება ავლენს სპეციფიკურ ხასიათს, ვინაიდან რეაქციის მიმდინარეობისას ძირითად ოქსიდთან (Cr_2O_3) ერთად ადგილი აქვს ქრომიტის ($LaCrO_3$) წარმოქმნასაც, რომელიც ქმნის დიფუზიურ ბარიერებს. ყოველივე ეს იწვევს ოქსიდირების კინეტიკის გადახრას პარაბოლური კანონისაგან. FeCr შენადნობის იტრიუმით ლეგირებისას წარმოიქმნება შესაბამისი ქრომიტი ($YCrO_3$), რომელიც ასევე ქმნის დიფუზიურ ბარიერებს და ცვლის ოქსიდირების კინეტიკის პარაბოლურ ხასიათს. ვინაიდან FeCr(Ce) შენადნობის ოქსიდირების კინეტიკა FeCr(La) და FeCr(Y) შენადნობების ოქსიდირების კინეტიკის ანალოგიურია, გამოთქმულია ვარაუდი, რომ ამ შემთხვევაშიც ადგილი აქვს დიფუზიურ ბარიერებს ქრომიტ $CeCrO_3$-ის სახით.

REFERENCES

1. Nakhutsrishvili I., Kokhreidze R. and Kakhniashvili G. (2022) Influence of the simultaneous processes of scale evaporation and reaction surface reduction on the oxidation kinetics of chromia-forming alloys doped with rare-earth elements. *Georgian Scient*., **4**: 141-146.
2. Tavadze F., Mikadze O., N.Keshelava N. and Bulia B. (1986) High-temperature corrosion of dilute chromium-lantanum alloys. *Oxidat. of Met*., **25**: 335-350.
3. Evans U.R. (1960) The corrosion and oxidation of metals: scientific principles and practical applications, 662 p., E.Arnold LTD, London.
4. Nakhutsrishvili I. (2006) New kinetic equation of scale growth with decrease of reaction surface. *Georgian Eng. News*, **4**: 134-136.
5. Mikadze O., Nakhutsrishvili I., Maisuradze N. and Mikadze G. (2007) Kinetic regularities of growth of scale on heat resisting alloys with barrier layers of stable oxides. *Metal Phys. and Adv. Technologies*, **29**: 1507-1513.
6. Nakhutsrishvil I., Mikadze O. and Mikadze G. (2007) Mutual connection of unisothermal initial heating with isothermal oxidation kinetics of heat-resistant chromium alloys. *Proc. Georgian Acad. Sci.,* **33**: 60-63.
7. Pillis M.F., Correa O.V. and Ramanathan L.V. (2016) High temperature oxidation behavior of yttrium dioxide coated Fe-20Cr alloy. *Materials Res*., **19**: 611-617.
8. Fontana S., Vuksa M., Chevalier S., Caboche G. and Piccardo P. (2008) On the effect of surface treatment to improve oxidation resistance and conductivity of metallic interconnects for SOFC in perating conditions. *Mater. Sci. Forum*, **595/598**: 753-762.
9. Sayto Y. (1989) Effects of rare earth elements on the high temperature oxidation of heat-resistant alloys. In: Studies in Organic Chemistry, 391 p., Elsevier, Amsterdam-Oxford-New York-Tokyo.
10. Molin S., Persson A.H., Skafte T.L., Smitshuysen A.L., Jensen S.H., Andersen K.B., Xu H. and Chen M. (2019) Effective yttrium based coating for steel interconnects of solid oxide cells: corrosion evaluation in steam-hydrogen atmosphere. *Power Sources*, **440**: article id. 26814.
11. Downham D.A., Hussey R.J., Mitchell D.F. and Graham,M.J. (1990) Segregation of cerium in chromia scales. Proc. Int. Symp. on high-temperature oxidation and sulphidation processes, 101-106. Hamilton, Ontario, Canada, August 26-30.
12. Li H., Cui X and Chen W. (2011) Mechanism of coke formation caused by catalytic nanochromium carbide particles from decomposition of $CeCrO_3$. *Amer. Cer. Soc*., 94: 2578-2584.
13. Mikkelsen L. and Linderoth S. (2003) High temperature oxidation of Fe–Cr alloy in O_2–H_2H_2O atmospheres; microstructure and kinetics. *Materials Sci. and Eng. A*, **361**: 198-212.
14. Rhis-Jones T.N., Grabke H.J. and Kudielka H. (1987) The high temperature oxidation of iron-chromium alloys containing 0.1 wt. % cerium or cerium oxide. *Materials and Corros*.,3: 65-72.
15. Tufiq Jamila M. , Ahmada J., Hamad Bukharia S. and Saleemb M. (2018) Effect of Re and Tm-site on morphology structure and optical band gap of $ReTmO_3$ (Re = La, Ce Nd, Gd, Dy, Y and Tm = Fe, Cr) prepared by sol-gel method. *Rev. Mex. de F´isica*, **64**: 381-391.

Received September, 2022